Aliasing separation in accelerated MR image acquisition by voxel modification

Min-Oh Kim[1], Joonsung Lee[1], Sang-Young Zho[1], and Dong-Hyun Kim[1]
[1]*Electrical and Electronic Engineering, Yonsei University, Seoul, Korea, Republic of*

Introduction One acquisition time reducing technique called simultaneous multi-slice acquisition [1] uses simultaneous multi-slice excitation and separates multiple slices by additional gradient along slice direction. This concept has been successfully applied to wideband MRI [2]. These methods have focused on through-plane acceleration by acquiring multiple planes at once. Here, we modified this approach to single slice 2D imaging acceleration and merged it to 3D imaging acceleration along both in-plane and through-plane phase encoding (PE) directions. In contrast to the previous works, the proposed method does not require special RF pulses like simultaneous multi-slice/slab excitation and can accelerate along in-plane and/or through-plane PE directions selectively.

Methods Conventional gradient echo (GRE) pulse sequence is modified as Fig. 1. Aliasing artifacts resulting from PE-undersampling in G_{SS} and/or G_{PE} are separated to RO direction by applying $G_{SS.sep}$ and/or $G_{PE.sep}$ along the undersampled direction during RO time. The concept of aliasing separation is illustrated in Fig. 2.

For 2D imaging acceleration, we define the aliasing separation distance as $d_{sep} = R_{PE} \cdot FOV_{G_{PE}}$, where R_{PE} is the ratio of $G_{PE.sep}$ over G_{RO} and $FOV_{G_{PE}}$ is the field-of-view along G_{PE} direction with undersampling. If the longest object length along RO direction l_{max} is considered as the minimum separation distance for image without aliasing artifacts, then the required $R_{PE} = l_{max}/FOV_{G_{PE}}$. According to this relation, higher acceleration is achieved by larger R_{PE}. In other words, bigger $G_{PE.sep}$ is needed for higher acceleration. For acceleration in both PE directions in 3D imaging, proportionally bigger $G_{SS.sep}$ compared to $G_{PE.sep}$ is required because l_{max} is re-defined after 2D acceleration as $l'_{max} = l_{max} \cdot W_{PE}$ where W_{PE} is acceleration factor along G_{PE} direction. So, $R_{SS} = l'_{max}/FOV_{G_{SS}}$ is required for alias-free accelerated 3D images.

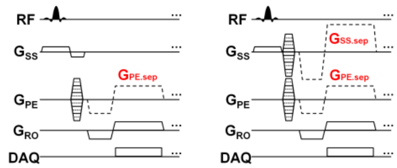

Figure 1. Pulse sequence diagram for 2D (right) and 3D (left) acceleration. The phase-encoding gradient and the pre-phasing gradient in G_{SS} and G_{PE} can be merged to optimize the pulse sequence.

With this acquisition method, voxel is modified to sheared form as illustrated in Fig. 3. The amount of shearing depends on R and resolutions along RO and PE direction. As shown in Fig. 3 left, bigger R for higher acceleration makes voxel more sheared which results in more blurring artifact. On the other hand, better PE resolution compared to RO resolution can reduce the amount of blurring as illustrated in Fig. 3 right. In k-space perspective, FOV and resolution are re-defined with respect to the sampling trajectory of the proposed method which samples k-space diagonally with slope R. Along a diagonal direction k_{diag1} with slope R, $k_{diag1.max}$ and Δk_{diag1} are $(R^2+1)^{1/2}$ $k_{RO.max}$ and Δk_{RO} respectively. This causes increment of resolution corresponds to k_{diag1} and reduction of FOV_{diag1} which can be compensated by readout oversampling. On the other hand, along the other diagonal direction k_{diag2} with slope $-1/R$, $k_{diag2.max}$ and Δk_{diag1} are $(R^2+1)^{-1/2}$ $k_{PE.max}$ and Δk_{PE} respectively. This causes loss of resolution corresponds to k_{diag2} and increment of FOV_{diag2} where the aliasing artifacts are separated. The anisotropic diagonal resolutions of sheared voxels are noted at Fig.3. In summary, aliasing artifacts are resolved by the increased diagonal FOV at the cost of partial diagonal resolution loss according to the gradient ratio R.

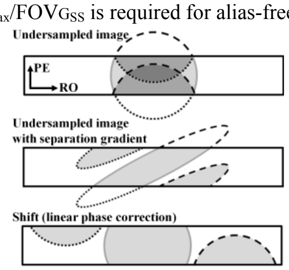

Figure 2. Conceptual illustration of aliasing separation. To get a clear image, linear phase correction is applied

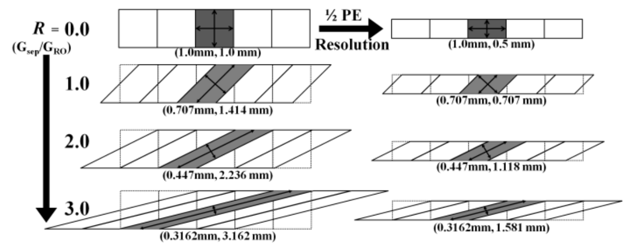

Figure 3. Voxel modifications according to R (rows) and resolution (columns) along phase-encoding direction. The diagonal lengths of sheared voxels are noted.

Experiments were performed on Siemens 3T Tim Trio scanner using a manually designed grid phantom and invivo. The scan parameters for the single slice phantom imaging TR = 30ms / TE = 9.8ms / $R_{PE.sep}$= 0, 2, 3, 4, 5, 6 / W_{PE} = 0, 2, 3, 4, 5, 6 / resolution 1.0 x 1.0 x 2.0 mm^3 / measured matrix size (RO x PE) = 1536 x [256, 128, 88, 64, 48, 40] / final matrix size = 256 x 256 / total acquisition time = 7.68, 3.84, 1.92, 1.32, 0.96, 0.72, 0.60s, and for invivo imaging were TR=30ms / TE=9.8ms / $R_{PE.sep}$=1.5 / $R_{SS.sep}$=3 / W = 6 (W_{PE} = 2, W_{SS} = 3) / resolution = 1.0 x 1.0 x 0.5 mm^3 / measured matrix size (RO x PE x Slice) = 1152 x 96 x 192 / final matrix size = 192 x 192 x 576 / total acquisition time = 9m 13s.

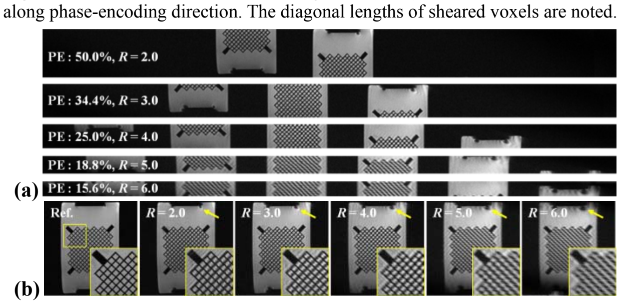

Figure 4. (a) Acquired phantom images with increasing undersamping (acceleration) factor from top to bottom. The sampling percentages and R values are noted. **(b)** Reference image without acceleration and reconstructed images of (a). Yellow boxed region is magnified to visualize sheared voxel characteristic more effectively. Increment of T2* effect with R is indicated by yellow arrow.

Results and Discussion The acquired and reconstructed phantom images with varying undersampling ratios are shown in Fig. 4. These images show the relationship between acceleration and blurring. As expected, higher acceleration causes more blurring, but the blurring pattern is anisotropic due to the sheared voxel characteristic as explained before and depicted in Fig. 3. Because of this anisotropic diagonal resolution characteristic, imaging with high acceleration factor could be useful for increasing temporal resolution in line tagged cardio-vascular imaging. In addition to the sheared voxel characteristic, T2* effect due to the applied separation gradient is increased along the increment of R and this phenomenon is indicated by yellow arrows in Fig. 4(b). The acquired invivo images with 6X acceleration and the reconstruction procedures are shown in Fig. 5(a). The aliasing-separated images are merged into in-plane and through-plane sequentially. The final images in Fig. 5(b) show little blurring because the minimum separation gradients (R_{PE}=1.5, R_{SS}=3.0) were applied and the slice thickness was half of the readout resolution (1.0 x 1.0 x 0.5 mm^3). Apart from the sheared voxel characteristic and T2* effect, several more factors should be considered for application in higher acceleration. These issues include SNR loss due to undersampling and gradient hardware limitation. When G_{sep} with maximum power is not enough to make desired R, G_{RO} should be decreased and it causes reduction of RO bandwidth and increment of TE_{min}.

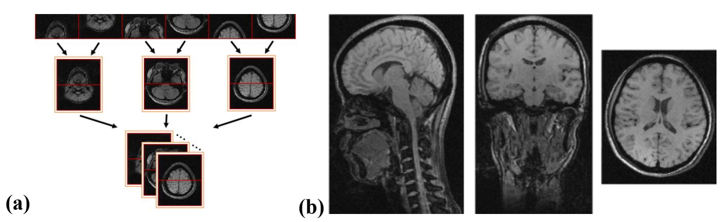

Figure 5. Invivo 3D imaging result with 6X acceleration, 2X along in-plane PE and 3X along through-plane PE. **(a)** Acquired image (top) and reconstruction procedures in in-plane (middle) and through-plane (bottom). **(b)** Final images with sagittal, coronal and axial views.

Conclusion By applying separation gradients along both PE directions in 3D MR imaging**,** aliasing artifacts caused by PE-undersampling are successfully separated and 6X acceleration is achieved in invivo high-resolution 3D MR imaging. This technique can be applied to not only gradient echo sequences but also spin echo based sequences. For further acceleration, the proposed method can be combined with parallel imaging techniques which has been successfully applied in through-plane acceleration methods such as simultaneous parallel inclined readout image technique [3] and wideband MRI [4]. Despite these high acceleration capability, some limitations such as sheared voxel characteristic, maximum gradient limitation, T2* effect and SNR loss exist.

Acknowledgement Korea MKE and KIAT through the Workforce Development Program in Strategic Technology, KOSEF grant No. 2011-0002495.

References **[1]** Weaver, MRM., 8:275-284, 1988 **[2]** Wu, ISMRM., p2678, 2009 **[3]** Martyn, MRI., 24:557–562,2006 **[4]** Wu, ISMRM., p2677, 2009